

Analysis of Settlements Induced by the Excavation of a Cross passage Using 2D and 3D Numerical Modeling

I. Siad & M. Akchiche

LEEGO Laboratory of Civil Engineering Faculty, USTHB Bab Ezzouar, Algiers, Algeria

P. Spyridis

Faculty of Agricultural and Environmental Sciences, Rostock Univ, Rostock, Germany

Abstract: The construction of cross passages, which are connecting structures between two adjacent tubes or between a tube and a ventilation shaft causes in most of the cases deformations in the main tunnel lining as well as in the soil surface. In this paper, we will investigate the effect of excavating a cross passage on the main tunnel, by simulating the excavation of the two galleries separately in 2D and 3D using the CESAR LCPC calculation code, and comparing the results with the 3D numerical model that combines the two galleries.

Keywords: Cross Passage, 2D numerical modeling, 3D numerical modeling, CESAR LCPC, Surface Settlement.

1. INTRODUCTION

Tunnel intersections are the structurally weakest regions of underground openings, and instabilities can occur in these regions. Furthermore, the structural mechanism of tunnel intersections is not yet well understood. Despite their importance and complexity, there are relatively few publications and methods concerning the design of tunnel intersections Gercek (1986).

In spite of the fact that tunnel excavation is a complex three-dimensional problem, experience acquired on tunnel projects has shown that the results obtained with two-dimensional, plane deformation models are quite satisfactory Do et al (2014), Vlachopoulos et al (2014). In most cases, calculations are based on the principle of convergence confinement. Generally, a single tunnel cross section can be regarded as a 2D plane strain problem, as the length of the tunnel is significantly larger than its cross-section dimensions, and therefore the problem geometry can be regarded as constant in the out-of-plane axis. Conversely, the intersection of two tunnels is essentially a 3D problem. Some researchers have previously adopted photoelastic methods to study the stress concentration factor at tunnel intersections, e.g. Riley (1964), Pant (1971). Subsequently, the rapid development of numerical modeling techniques enabled 3D analysis to be used more widely by researchers to analyze the stresses and deformations of underground excavations whether it be with BEM Beer et al (1987) or even FEM Tsuchiyama et al (1988) Pöttler (1992).

Though 3D programs have become more accessible, they remain a limited tool for practical applications. Not only are they costly in terms of calculation time, but building a 3D model requires considerable expertise in the software used. For this reason, we have proposed in this work to perform 2D numerical models that consider the construction of the main tunnel and the cross passage separately, and then compare the results in terms of surface settlement with the results of 3D numerical modeling, which takes into account the globality of the 3D problem and allows more precise consideration of the geometry of the intersection problem, both the 2D models and the 3D model were performed using the CESAR LCPC calculation code.

2. METHODOLOGY

2.1 2 D numerical calculation

The two-dimensional models of the main tunnel Fig 1. (a) and the cross passage Fig 1. (b) were carried out using the CESAR LCPC V5 2D computational code. Considering the symmetry of the problem, only half a section of the tunnel geometry is modeled. The cover above the main tunnel is 20 m.

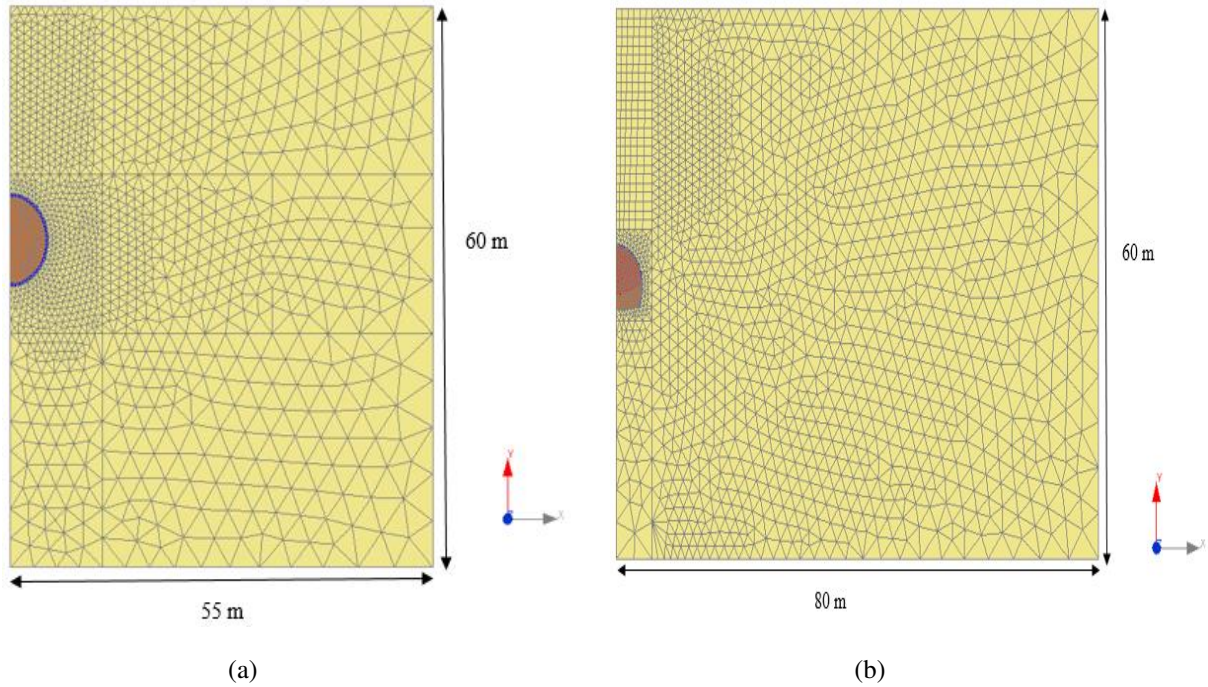


Figure 1. Geometry and mesh in 2D: (a) Main tunnel, (b) Cross passage

The calculations were carried out considering an elastoplastic behavior for the soil with the Mohr Coulombs behavior law, while the support elements are modeled as a linear elastic material. The mesh of the main tunnel model comprises around 722 triangular elements and 1362 nodes. And that of the connecting branch comprises 353 triangular elements and 654 nodes. For the boundary conditions, lateral and vertical displacements are blocked ($U = 0$, $V = 0$) and only surface displacements are allowed.

It was assumed that the main tunnel would be driven by a tunnel boring machine (TBM), while the cross passage would be built using the NATM technique. This applies to both 2D and 3D calculations

The simulation of the cross passage tunneling was carried out in different phases. The executive phasing adopted in the following calculation has tried to reproduce, as faithfully as possible, the various stages of constructive phasing associated with the main tunnel and cross passage tunneling in a current situation. The phasing of the calculations is summarized in the following tables:

Table 1. Calculation phase for the 2D main tunnel

Step	Description
0	Constraint initialization
1	Excavation of the entire tunnel cross-section and deconfinement of $\lambda_1 = 0.55$ with pressure applied to the front face
2	Installation of 0.45 cm thick support and deconfinement of $\lambda_2 = 0.45$

Table 2. Calculation phase for the 2D cross passage

Step	Description
0	Constraint initialization
1	Excavation of the upper section and deconfinement of $\lambda'_1 = 0.6$
2	Installation of 0.23 cm thick support and deconfinement of $\lambda'_2 = 0.4$
3	Excavation of the lower section and deconfinement of λ'_1
4	Installation of 0.23 cm thick support and deconfinement of λ'_2

2.2 3D numerical calculation

The geometric model of the tunnel-cross passage intersection considered in this study is shown in Figure 2, with an aspect ratio of $d/D = 0.8$. The main tunnel has a circular shape with a diameter of $D = 10$ m, while the connecting branch has a horseshoe shape with an equivalent diameter of $d = 8$ m. In order to neglect the influence of boundary effects, the model dimensions are set at 160 m in the longitudinal direction Y (direction of excavation) and transverse X is 110 m and 60 m in depth. The cover over the main tunnel is 20 m as shown in Figure 2. The lining of the main tunnel and connecting branch was modeled using volume elements. In the end, the number of mesh zones is around 22045, with 130714 nodes.

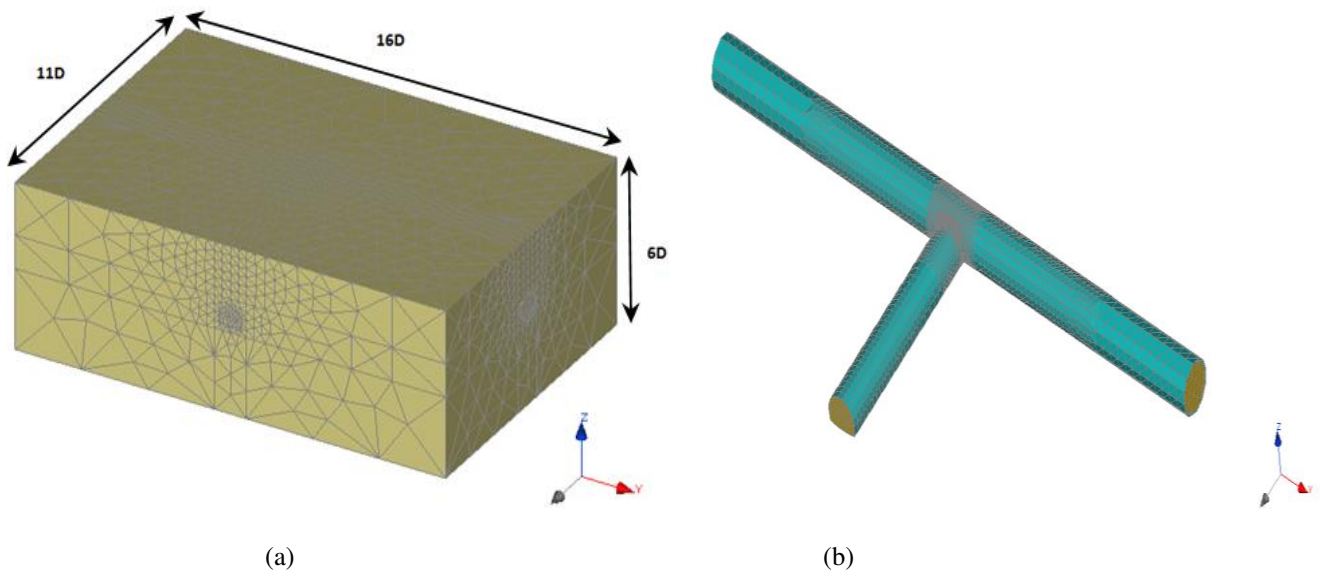


Figure 2. Three-dimensional numerical model: (a) Isometric view; (b) Relative positions of main tunnel and cross passage

The main tunnel lining is composed of continuous elements with a constant thickness of 45 cm. The cross passage lining is made up of arches and shotcrete. In the model, it is homogenized and has a thickness of 23 cm. The behavior of the soil mass was assumed to be governed by an elastoplastic constitutive model based on the Mohr-Coulomb failure criterion with a non-associative flow rule. While the supporting elements are modeled as a linear elastic material. Concerning boundary conditions, the numerical model background is blocked in all three directions (X, Y, Z), while only horizontal movements are fixed on the lateral faces. More details are exposed in table 3.

Table 3. Geomechanical characteristics used in 3D modeling

Parameter	Marne	Main tunnel lining	Cross passage lining
Density (Kn/m ³)	21	/	/
Elastic modulus (MPa)	111	35000	25000
Poisson's ratio	0.3	0.2	0.2
Cohesion (KPa)	56	/	/
Friction angle (°)	21	/	/
Angle of dilatation (°)	10	/	/

The following table Tab 4 details the phasing adopted for the construction of the main tunnel the cross passage in 3D.

Table 4. 3D numerical model calculation steps

Step	Description
0	Generation of initial stresses with a resting earth coefficient equal to 0.6. This value defines the stress anisotropy in the initial state.
1	Excavation of the entire cross-section of the main tunnel and deconfinement of $\lambda_1=0.55$ with application of a trapezoidal pressure to the face, so the value of the mean face pressure (applied to the tunnel axis) is generally equal to the horizontal ground pressure $P_{front} = 0.252$ MPa.
2	Installation of a 0.45 cm thick support and deconfinement of $\lambda_2=0.45$.
From 3 to 62	Excavation and application of the main tunnel lining.
63	Digging of the cross passage opening and application of a deconfinement factor of $\lambda=0.35$
64	Activation of the support corresponding to the previous phase and application of a deconfinement factor of $\lambda=0.65$
65	Excavation of the upper half section and deconfinement of $\lambda_1=0.6$
66	Installation of a 0.23 cm thick support and deconfinement of $\lambda'_2=0.4$.
From 67 to 116	Excavation and application of the cross passage lining.

3. RESULTS AND DISCUSSION

- 2D calculation

Figures 3.a and 3.b illustrate the surface settlement obtained after the excavation of the main tunnel and the cross passage. A preliminary analysis of the curves shows that the settlement values obtained reach a value of $U_z = -5.166$ mm and $U_z = -15.9$ mm for the tunnel and cross passage respectively.

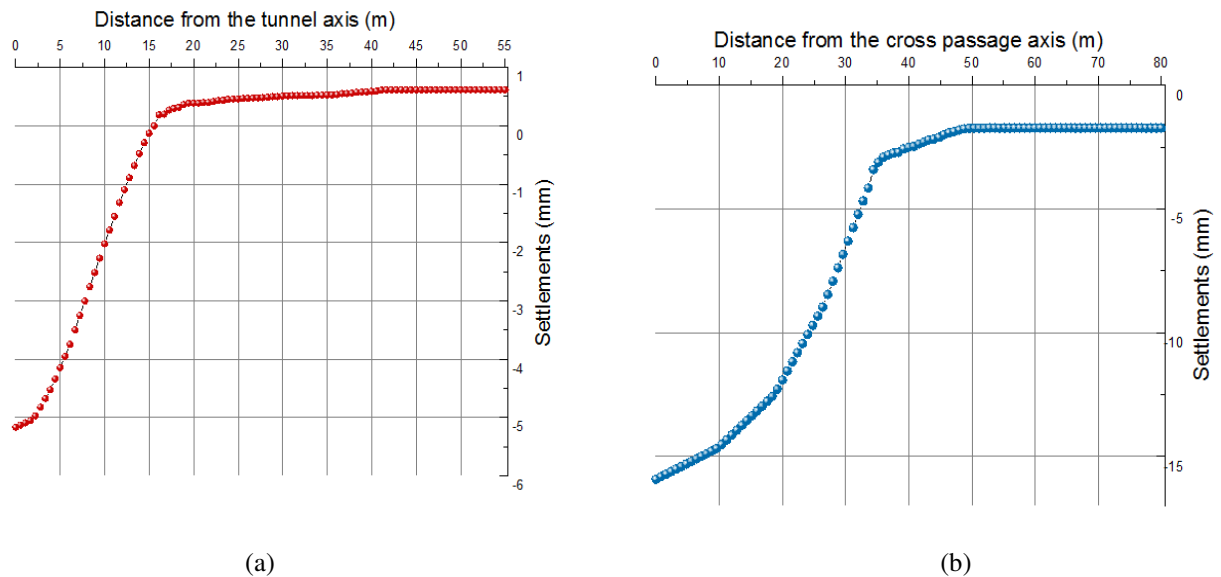


Figure 3. 2D surface settlement : a) Main tunnel, b) Cross passage

- 3D calculation

Figure 4 shows the results of surface settlement after excavation of the main tunnel, followed by excavation of the lateral opening and complete excavation of the cross passage.

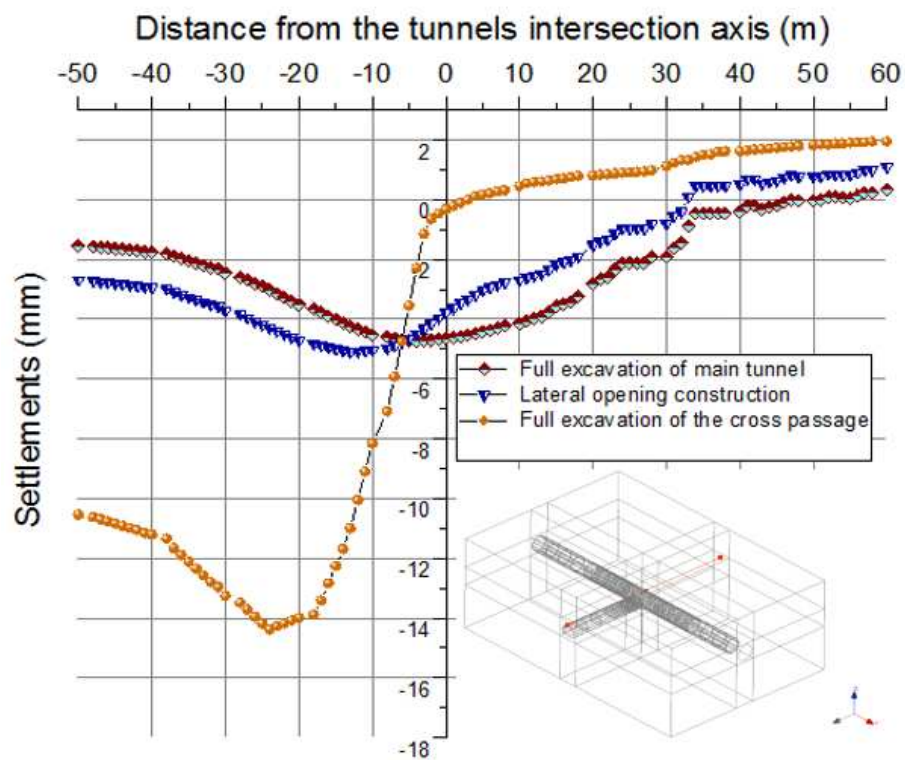


Figure 4. Settlement trough before and after excavating the cross passage

The following figure shows the surface settlement results obtained after digging the cross passage alone in 3D.

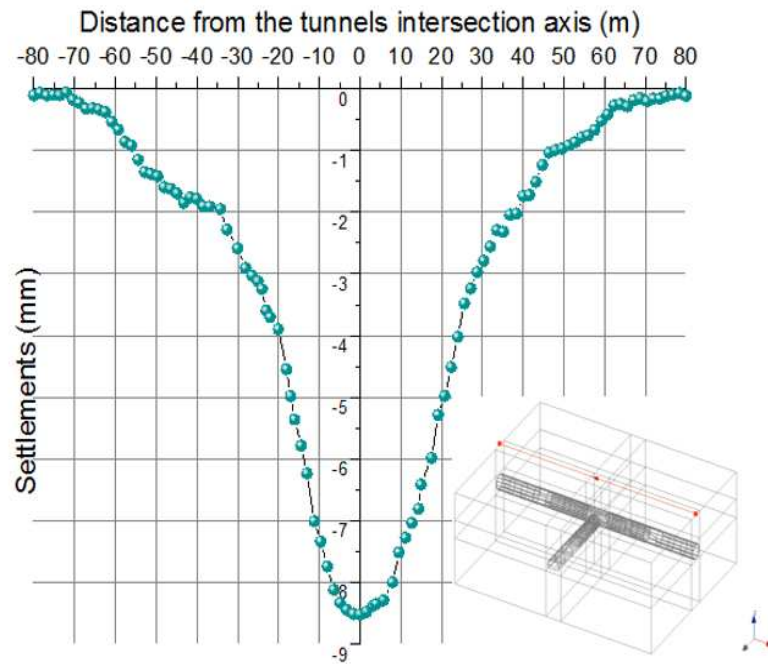


Figure 5. Surface settlement caused by excavation of the cross passage

4. SUMMARY OF RESULTS

Table 5. Summary of 2D and 3D calculation results

	2D calculation	3D calculation
Tunnel	5.166 mm	4,65 mm
Cross passage	15,9 mm	8,25 mm
Tunnel+ Cross passage	/	14.38 mm

Although the results of the 2D calculation may not be very significant in the case of a tunnel intersection, they can give an order of magnitude of the settlement values induced. The sum of the settlements induced by the 2D calculation of the tunnel and the cross passage yields a value equivalent to 21 mm, which is higher than the value obtained in 3D, equal to 14.38 mm. This is quite obvious, given that the 2D calculation does not represent the real problem of the excavation studied.

When each of the tunnels was modelled separately in 3D (Fig 4 and Fig 5), the settlement values showed a variance between $U_z = -4.65$ mm and $U_z = -8.25$ mm for the main tunnel and the cross passage respectively. This implies that the sum of the two values gives us a slightly lower value than that obtained when excavating the main tunnel and the cross passage in a single model. This is due to the fact that excavation of the main tunnel causes plasticization and stress reduction in the soil, so that when the cross passage is subsequently excavated in the same numerical model, settlement increases rapidly compared with the excavation of the two tunnels separately. It can also be seen that the value of surface settlement caused by the excavation of the cross passage alone is significantly higher than that obtained by the excavation of the main tunnel alone. This is due to the front pressure applied to the main tunnel, which ensures tunnel stability and reduces surface settlement.

5. CONCLUSION

In this study we compared 2D and 3D models of a cross passage excavation from a main tunnel in terms of surface settlements, the results showed that the 2D approach gives slightly higher settlement values than the 3D model, and then excavating each gallery separately gives a lower total settlement value than excavating the galleries in a single model. This is due to the plasticization and stress reduction caused by excavation of the main tunnel. In conclusion, the 3D approach gives more realistic results, due to the accurate representation of the geometry of the problem.

6. REFERENCES

- Beer, G. Watson, J. O., Swoboda, G. (1987). Three-dimensional analysis of tunnels using infinite boundary elements. *Computers and Geotechnics*, 3(1), pp.37–58.
- Do, N. A., Dias, D., Oreste, P., & Djeran-Maigre, I. (2014). 2D tunnel numerical investigation: the influence of the simplified excavation method on tunnel behaviour. *Geotechnical and Geological Engineering*, 32, 43-58.
- Gerçek, H. (1986). Stability considerations for underground excavation intersections. *Mining Science and Technology*, 4(1), pp.49–57.
- Pant, B. 1971. Analysis and design of pressure tunnel intersection. Indian Society of Engineering Geology, *Tunnelling Seminar*, Part 1.
- Pöttler, R. (1992). Three-dimensional modelling of junctions at the Channel Tunnel project. *International Journal for Numerical and Analytical Methods in Geomechanics*, 16(9), pp.683–695.
- Riley, W. F. (1964). Stresses at Tunnel Intersections. *Journal of the Engineering Mechanics Division*, 90(2), pp.167–179.
- Tsuchiyama, S., Hayakawa, M., Shinokawa, T., Konno, H. (1988). Deformation behavior of the tunnel under the excavation of crossing tunnel. *Proceedings of the sixth international conference on numerical methods in geomechanics*, Volumes1-3.
- Vlachopoulos, N., & Diederichs, M. S. (2014). Appropriate uses and practical limitations of 2D numerical analysis of tunnels and tunnel support response. *Geotechnical and Geological Engineering*, 32, 469-488.

INTERNATIONAL SOCIETY FOR SOIL MECHANICS AND GEOTECHNICAL ENGINEERING



This paper was downloaded from the Online Library of the International Society for Soil Mechanics and Geotechnical Engineering (ISSMGE). The library is available here:

<https://www.issmge.org/publications/online-library>

This is an open-access database that archives thousands of papers published under the Auspices of the ISSMGE and maintained by the Innovation and Development Committee of ISSMGE.

The paper was published in the proceedings of the 18th African Regional Conference on Soil Mechanics and Geotechnical Engineering and was edited by Abdelmalek Bekkouche. The conference was held from October 6th to October 9th 2024 in Algiers, Algeria.